

Degenerate polarization entangled photon source based on a single Ti-diffusion lithium niobate waveguide in a polarization Sagnac interferometer

Yu Sun(孙宇), Chang-Wei Sun(孙昌伟), Wei Zhou(周唯), Ran Yang(杨然),Jia-Chen Duan(端家晨), Yan-Xiao Gong(龚彦晓), Ping Xu(徐平), and Shi-Ning Zhu(祝世宁)

Citation: Chin. Phys. B, 2023, 32 (**8**): 080308. DOI: 10.1088/1674-1056/acd8b3
Journal homepage: http://cpb.iphy.ac.cn; http://iopscience.iop.org/cpb

What follows is a list of articles you may be interested in

Algorithm for evaluating distance-based entanglement measures

Yixuan Hu(胡奕轩), Ye-Chao Liu(刘烨超), and Jiangwei Shang(尚江伟)
Chin. Phys. B, 2023, 32 (**8**): 080307. DOI: 10.1088/1674-1056/acd5c5

Circuit quantum electrodynamics with a quadruple quantum dot

Ting Lin(林霆), Hai-Ou Li(李海欧), Gang Cao(曹刚), and Guo-Ping Guo(郭国平)
Chin. Phys. B, 2023, 32 (**7**): 070307. DOI: 10.1088/1674-1056/accd57

Anomalous non-Hermitian dynamical phenomenon on the quantum circuit

Chenxiao Dong(董陈潇), Zhesen Yang(杨哲森), Jinfeng Zeng(曾进峰), and Jiangping Hu(胡江平)
Chin. Phys. B, 2023, 32 (**7**): 070305. DOI: 10.1088/1674-1056/acce9a

First-order quantum phase transition and entanglement in the Jaynes-Cummings model with a squeezed light

Chun-Qi Tang(汤椿琦) and Li-Tuo Shen(沈利托)
Chin. Phys. B, 2023, 32 (**7**): 070303. DOI: 10.1088/1674-1056/acb9f0

Energy shift and subharmonics induced by nonlinearity in a quantum dot system

Yuan Zhou(周圆), Gang Cao(曹刚), Hai-Ou Li(李海欧), and Guo-Ping Guo(郭国平)
Chin. Phys. B, 2023, 32 (**6**): 060303. DOI: 10.1088/1674-1056/acc521

RAPID COMMUNICATION

Degenerate polarization entangled photon source based on a single Ti-diffusion lithium niobate waveguide in a polarization Sagnac interferometer

Yu Sun(孙宇)[1], Chang-Wei Sun(孙昌伟)[2], Wei Zhou(周唯)[1], Ran Yang(杨然)[1], Jia-Chen Duan(端家晨)[1], Yan-Xiao Gong(龚彦晓)[1], Ping Xu(徐平)[3,†], and Shi-Ning Zhu(祝世宁)[1]

[1] *National Laboratory of Solid State Microstructures and School of Physics, Nanjing University, Nanjing* 210093, *China*
[2] *NanZhi Institude of Advanced Optoelectronic Integration, Nanjing* 210018, *China*
[3] *Institute for Quantum Information and State Key Laboratory of High Performance Computing, College of Computer Science and Technology, National University of Defense Technology, Changsha* 410073, *China*

(Received 11 May 2023; revised manuscript received 11 May 2023; accepted manuscript online 25 May 2023)

Combining a Ti-diffusion periodically poled lithium niobate (PPLN) waveguide with a Sagnac interferometer, two opposite directions type-II spontaneous parametric down conversions (SPDC) occur coherently and yield a high brightness, high stability polarization entanglement source. The source produces degenerate photon pairs at 1540.4 nm with a brightness of $B = (1.36 \pm 0.03) \times 10^6$ pairs/(s·nm·mW). We perform quantum state tomography to reconstruct the density matrix of the output state and obtain a fidelity of $F = 0.983 \pm 0.001$. The high brightness and phase stability of our waveguide source enable a wide range of quantum information experiments operating at a low pump power as well as hold the advantage in mass production which can promote the practical applications of quantum technologies.

Keywords: polarization entanglement source, Sagnac interferometer, quantum information, lithium niobate waveguide

PACS: 03.65.Ud, 03.67.–a, 42.50.Dv, 42.65.–k **DOI:** 10.1088/1674-1056/acd8b3

1. Introduction

Polarization entangled photons are crucial quantum resources for various applications in quantum information, such as quantum key distribution,[1–4] quantum computing,[5–8] and teleportation.[9–11] To achieve high brightness, stability, and entanglement purity, various methods have been employed for generating polarization entangled photons. The first practical solution for preparing a polarization entangled light source utilizes β-barium-borate (BBO) crystals, which produces polarization entangled photon pairs emitted at the intersection of two conical surfaces.[12] With advancements in nonlinear optics, periodic poling (pp) of nonlinear crystals considerably relaxes the phase-matching conditions for spontaneous parametric down conversion (SPDC) by enabling quasi-phase-matching (QPM) and allows full exploration of the material's nonlinear properties.

In the past few decades, various schemes have emerged for generating polarization entanglement using periodically poling bulk crystals or waveguide structures. For instance, one approach involves combining two co-linear SPDC processes,[13,14] or designing a dual-period structure that generates two SPDC processes simultaneously.[15–17] The photons generated by these methods can be split using a dichroic mirror (DM) or polarizing beam splitter (PBS). Some schemes use a dual-channel structure to combine two SPDC processes to generate a polarization entanglement source.[18–21] A more mature solution is to build the source using the Sagnac interferometer. This method generates polarization entanglement by creating a temporally distinguishable superposition of orthogonally polarized identical photon pairs and then removing that temporal delay. The Sagnac structure has been widely used to generate polarization entangled sources because the two SPDC processes come from opposite directions of the same periodically polarized crystal. Compared to the dual-structure, this method ensures that the parametric spectra of the two processes coincide exactly and that the relative phases of the two processes are very stable. The original scheme for generating polarization entanglement using the Sagnac interferometer involved a type-I down-conversion process in BBO crystals.[22] However, this source suffered from a 50% photon loss rate due to the use of a pump beam splitter to separate the output photon pairs. Since then, a variety of schemes for Sagnac polarization entanglement sources have been proposed.[22–25] Benefiting from longer crystal lengths and higher nonlinearity, the brightness of polarization entanglement sources at a given pump light intensity has been increasing in recent years. To further improve the brightness, experiment[26] has been conducted to design a non-collinear type-I SPDC in periodically poled $KTiOPO_4$ (PPKTP). However, it is difficult to obtain a significant increase in the brightness of a polarization entan-

†Corresponding author. E-mail: pingxu520@nju.edu.cn

© 2023 Chinese Physical Society and IOP Publishing Ltd

glement source based on a bulk crystal.

In this paper, we adopt a Ti-diffusion periodically poled lithium niobate (PPLN) waveguide for the first time into a Sagnac interferometer to produce a higher brightness degenerate polarization entanglement source in the telecom regime. The brightness of the source reaches $(1.36\pm0.03)\times 10^6$ pairs/(s·nm·mW) and the polarization entanglement state violates Bell's inequality by 36 standard deviations with $S=2.76\pm0.02$.

2. Theory

We utilize QPM type-II SPDC process as the foundation of our source. In the type-II SPDC process, energy conservation and momentum conservation should be met, which are given by

$$\omega_{\rm p}=\omega_{\rm o}+\omega_{\rm e}, \tag{1}$$

$$k_{\rm p}=k_{\rm o}+k_{\rm e}+G_m. \tag{2}$$

The subscripts p, o and e represent the pump, signal and ideal photons, respectively. The reciprocal vectors (G_m) have the form

$$G_m=\frac{2\pi m}{\Lambda}, \tag{3}$$

where m represents the different orders of the reciprocal vectors and Λ is the poling period. We choose $m=1$ to utilize the maximal nonlinear coefficient. Assuming a pump at 780 nm, to generate degenerate down converted photon pairs at telecommunication band, the period is cited to be $\Lambda=9.07$ μm and the temperature is cited to 120 °C. The two-photon state produced by the SPDC process has the following form:

$$|\Psi\rangle=\Psi_0\int_{-\infty}^{\infty}{\rm d}\nu f(\nu)\hat{a}_{\rm s}^{\dagger}(\omega_{\rm o}^0+\nu)\hat{a}_{\rm i}^{\dagger}(\omega_{\rm e}^0-\nu)|0\rangle, \tag{4}$$

where ν represents the frequency detuning of the signal and idler photons. $f(\nu)$ denotes the spectral amplitude, which has the following form:

$$f(\nu)={\rm e}^{-{\rm i}\nu\tau/2}{\rm sinc}(\nu\tau/2),$$
$$\tau=L/\left(\frac{1}{u_{\rm s}}-\frac{1}{u_{\rm i}}\right), \tag{5}$$

where L is the length of the SPDC region and $u_{\rm s}$ and $u_{\rm i}$ are the group velocities of the signal and idler photons. The coefficient Ψ_0 absorbs all the constants which has the following form:

$$\Psi_0=\frac{{\rm i}E_{\rm p}Ld\pi}{\Lambda c}\sqrt{\frac{\omega_{\rm o}^0\omega_{\rm e}^0}{n_0n_{\rm e}}},$$

where $E_{\rm p}$ is the electrical field amplitude of pump, d is the effective nonlinear coefficient. $n_{\rm o}$ and $n_{\rm e}$ denote the refraction index of photons at frequency $\omega_{\rm o}^0$ and $\omega_{\rm e}^0$.

3. Experiment

According to the theoretical calculation, we fabricated a Ti-diffusion PPLN waveguide with SPDC region length of 350 mm and a poling period of 9.07 μm. Figure 1 shows the simulated mode field distribution of mode TM_0 in the waveguide by Lumerical simulation software. The mold field area is 66 μm^2. The waist area of a bulk LN crystal of the same length is about 2.7×10^5 μm^2. According to Eq. (4), the photon pair generation rate in Ti-diffusion LN waveguide is much higher than that in bulk crystal by three orders. To determine the wavelength of the pump light required for generating the degenerate spectrum and to test the nonlinear characteristics of the PPLN waveguide, we conducted second harmonic generation (SHG), a reverse process of SPDC. The SHG intensity with varied pump wavelength is recorded in Fig. 2. The full width at half maximum (FWHM) of the spectrum is 0.3 nm and the SHG process is phase matched at $\lambda=1540.5$ nm.

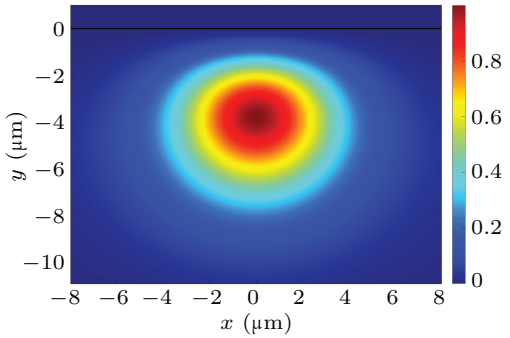


Fig. 1. The mode field distribution of mode TM_0 in the Ti-diffusion PPLN waveguide.

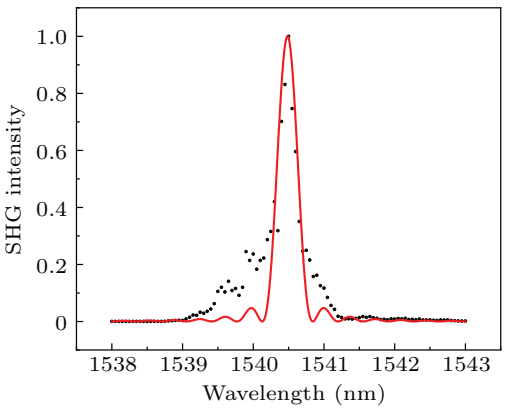


Fig. 2. SHG spectrum of the PPLN waveguide. The black dots correspond to SHG process at different wavelengths and the red line is a simulated curve.

The experimental setup is shown in Fig. 3. Here we generate a polarization entangled photon source with frequency degenerate at 1540.4 nm through this periodically poling titanium diffusion lithium niobate waveguide and a polarized Sagnac loop. A continuous-wave, single-frequency laser at 770.2 nm is used as the pump laser. Two aspherical mirrors (AM) with a focus length of 7.5 mm are used to focus the pump and collimate parametric light on the waveguide edge.

The polarized Sagnac interferometer consists of a dual wavelength polarizing beam splitter, a dual wavelength half-wave plate and two high reflecting ($R > 99\%$) mirrors at 770 nm and 1540 nm. The working principle of the device is described as follows. The pump is directed into the interferometer with a DM that is highly reflective for the pump and highly transmissive for the parametric light. The HWP_0 and QWP at 770 nm placed before the DM control the ratio and relative phase of the horizontal (H) and vertical (V) polarizations of the pumped light. The H-pump travelling in clock-wise direction in the Sagnac interferometer generates H and V polarized photons at 1540.4 nm through type-II quasi-phase-matched SPDC in the PPLN waveguide. The D-HWP plate transforms the polarization of both pump and SPDC photons from H to V and vice versa. Therefore, the down-converted H (V) polarized photons propagating in the clock-wise direction of the Sagnac interferometer are transformed into V (H) polarized photons and pass through the D-PBS. At the same time, the V-pump travelling in the counter clockwise on the Sagnac interferometer is transformed into H polarization after passing through the D-HWP plate and generates H and V polarized photons in the same PPLN waveguide. The photons generated in both clock-wise and counter clockwise directions of the Sagnac interferometer are combined by the D-PBS. It is well known that the sum of the phases of the photons generated through SPDC process equals the pump phase.[27] Since the clockwise and counter-clockwise pump lights pass through the same optical path in opposite directions, the polarization entangled photons generated by this scheme have ultra stable phases and are robust against any change in the optical path. The state combined by the D-PBS has the following form:

$$|\psi\rangle \propto \left(|H_s\rangle_1 |V_i\rangle_2 + e^{i\phi}\beta |V_s\rangle_1 |H_i\rangle_2\right),$$
$$\phi = \theta_s + \theta_i - \theta_p - \phi_p, \quad \beta = \frac{N_H}{N_V}, \tag{6}$$

where $\theta_s + \theta_i - \theta_p - \phi_p$ is the phases of the pump, signal and idler light introduced by the D-HWP, which will not vary in time and N_H/N_V is the photon generation rate ratio in both directions. After filtering the pump light with two high-pass filters, the 1540.4 nm photons emitted from the PBS are collected into the single-mode fiber through two high-reflectivity mirrors. The analyzer consisting of a HWP and a PBS is used to characterize the polarization entangled photons produced, where different HWP angles represent different measurements.

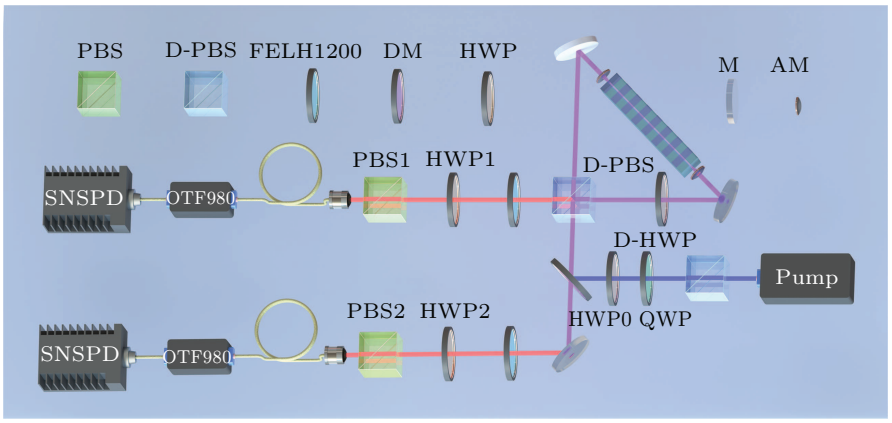


Fig. 3. The experimental setup. PBS: polarizing beam splitter, HWP: half wave plate, QWP: quarter wave plate, D-PBS: polarizing beam splitter at dual wavelengths, D-HWP: half wave plate at dual wavelengths, FELH-1200: long-pass filter, DM: dichroic mirror, AM: aspherical mirrors. HWP_0 and QWP are used to adjust the relative amplitude of the two counterpropagating down-conversion path and the phase of the output biphoton state.

4. Result

To verify that the SPDC process occurring in the waveguide produces degenerate polarized entangled photon pairs, we measured the central wavelengths of signal and idle photons at different pump wavelengths. Before the collected photons enter the superconducting single photon detector, the measured photon path is filtered with an adjustable filter (Santec710) with a bandwidth of 0.1 nm. By varying the center wavelength of the filter and measuring the coincidence count, the photon spectra of the signal and idler photons can be obtained. Ultimately, the signal photon and idler photon wavelengths are determined to be degenerate at 120 °C with a pump wavelength of 770.2 nm, and Fig. 4 illustrates the spectra of the signal and idler photons at this pump wavelength. The full width at maximum of the curve is 2.4 nm, and we confirmed the degenerate wavelength of the signal and idler photons to be $\Lambda = 1540.4$ nm. The side peaks in the spectrum are probably induced by fabrication errors, such as uneven width[28] or poling period.[29]

The next step is to characterize the quantum performances of the source. We measured the photon pair production rate at different pump powers with a 0.4 nm filter bandwidth at the central wavelength of 1540.4 nm, as shown in Fig. 5. The slope of the curve represents the photon pairs genera-

tion rate per unit pump power. The brightness of the source is $B = (1.36 \pm 0.03) \times 10^6$ pairs/(s·nm·mW). To assess the entanglement quality of the source, we performed a two-photon interference test on the source. Figure 6 shows the coincidence counts as a function of the angle of HWP_2 when the angle of HWP_1 is fixed at four different values 0°, 22.5°, 45°, and 67.5°. These four angles represent the four measurement bases H, V, D and A. In addition to the interference curve, the CHSH-type Bell inequality was also tested.[30] The measured S parameter is 2.76 ± 0.02 which confirms a strong violation of Bell inequality by 38 standard deviations.

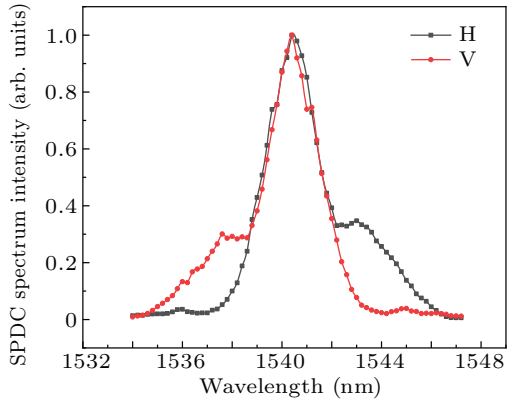


Fig. 4. The spectra of the degenerate photons. The black and red curves represent the spectra of H and V photons.

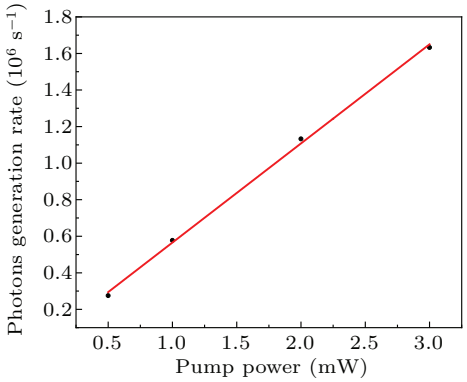


Fig. 5. Generation rate of photon pairs at different pumping powers.

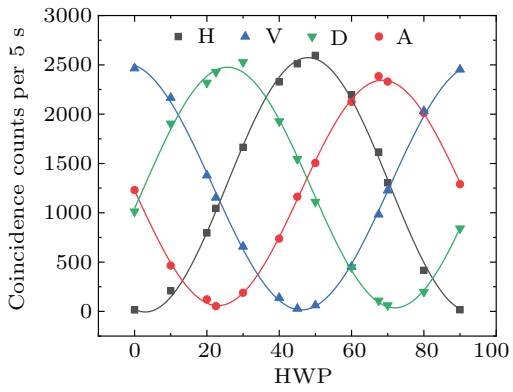


Fig. 6. Correlation measurements for four different bases: H/V (black/red) and diagonal D/A (blue/green).

Furthermore, in order to fully characterize our quantum state, we performed quantum tomography to reconstruct the density matrix,[31] with the real and imaginary parts shown in Fig. 7. The fidelity of the quantum state is $F(\varphi,\rho) = \langle\varphi|\rho|\varphi\rangle = 0.983 \pm 0.001$. These data demonstrate that the source is of high quality.

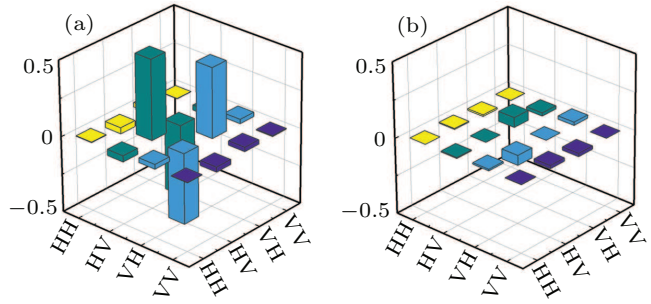


Fig. 7. (a) Real and (b) imaginary parts of the experimental density matrix of the state generated by our source.

5. Conclusion

In this paper, by using a type-II, degenerate SPDC process in a single PPLN waveguide with Sagnac interferometer, we produce a high brightness, high stability source of polarization entanglement. We evaluate the entanglement quality of the source through a two-photon interference test and achieve a high interference visibility and a fidelity of 0.983 ± 0.001. Furthermore, by measuring the CHSH inequality of the output state, we obtain an S value of 2.76 ± 0.02, violating the inequality by more than 38 standard deviations. Compared with the bulk schemes, the waveguide source has a stronger confinement to the light field and therefore allows more photons to be obtained at a lower pump power than the bulk system. Overall, our results demonstrate the high performance of our polarization entangled photon source, which has potential applications in quantum communication and information processing.

Acknowledgement

Project supported by the National Key R&D Program of China (Grant Nos. 2022YFF0712800 and 2019YFA0308700).

References

[1] Ekert A K 1991 *Phys. Rev. Lett.* **67**, 661
[2] Jennewein T, Simon C, Weihs G, Weinfurter H and Zeilinger A 2000 *Phys. Rev. Lett.* **84**,4729
[3] Liu H Y, Tian X H, Gu C S, Fan P F, Ni X, Yang R, Zhang J N, Hu M Z, Guo J, Cao X, Hu X P, Zhao G, Lu Y Q, Gong Y X, Xie Z D and Zhu S N 2021 *Phys. Rev. Lett.* **126**,020503
[4] Yin J, Cao Y, Li Y H, Liao S K, Zhang L, Ren J G, Cai W Q, Liu W Y, Li B, Dai H, Li G B, Lu Q M, Gong Y H, Xu Y, Li S L, Li F Z, Yin Y Y, Jiang Z Q, Li M, Jia J J, Ren G, He D, Zhou Y L, Zhang X X, Wang N, Chang X, Zhu Z C, Liu N L, Chen Y A, Lu C Y, Shu R, Peng C, Wang J Y and Pan J W 2021 *Science* **356**,1140
[5] Daniel G and Isaac L C 1999 *Nature* **402**, 390
[6] Knill E, Laflamme R and Milburn G J 2001 *Nature* **409**, 46
[7] Alberto P, Jonathan C F M and Jeremy L O B 2009 *Science* **325** 1221
[8] Jacob M, Nicholas C H, Gregory R S, Yoav L and Dirk E 2015 *Phys. Rev. A* **92** 032322

[9] Bennett C H, Brassard G, Crépeau C, Jozsa R, Peres A and Wootters W K 1993 *Phys. Rev. Lett.* **70** 1895

[10] Pirandola S, Eisert J, Weedbrook C, Furusawa A and Braunstein S L 2015 *Nat. Photon.* **9** 641

[11] Ren J G, Xu P, Yong H L, Zhang L, Liao S K, Yin J, Liu W Y, Cai W Q, Yang M, Li L, Yang K X, Han X, Yao Y Q, Li J, Wu H Y, Wan S, Liu L, Liu D Q, Kuang Y W, He Z P, Shang P, Guo C, Zheng R H, Tian K, Zhu Z C, Liu N L, Lu C Y, Shu R, Chen Y A, Peng C Z, Wang J Y and Pan J W 2017 *Nature* **549** 70

[12] Kwait P G, Mattle C, Weinfurter H, Zeilinger A, Sergienko A V and Shih Y H 1995 *Phys. Rev. Lett.* **75** 4337

[13] Ljunggren D, Tengner M, Marsden P and Pelton M 2006 *Phys. Rev. A* **73** 032326

[14] Suhara T, Nakaya G, Kawashima J and Fujimura M 2009 *IEEE Photonics Technology Letters* **21** 1096

[15] Thyagarajan K, Lugani J, Ghosh S, Sinha K, Martin A, Ostrowsky D B, Alibart O and Tanzilli S 2009 *Phys. Rev. A* **80** 052321

[16] Sun C W, Wu S H, Duan J C, Zhou J W, Xia J L, Xu P, Xie Z D, Gong Y X and Zhun S N 2019 *Opt. Lett.* **44** 5598

[17] Kuo P S, Verma V B and Nam S W 2020 *OSA Continuum* **3** 15

[18] Yosshizawa A and Tsuchida H 2004 *Appl. Phys. Lett.* **85** 2457

[19] König F, Mason E J, Wong F N C and Albota M A 2005 *Phys. Rev. A* **71** 033805

[20] Clausen C, Bussiéres F, Tiranov A, Herrmann H, Silberhorn C, Sohler W, Afzelius M and Gisin N 2014 *New J. Phys.* **16** 093058

[21] Sansoni L, Luo K H, Ricken R, Krapick S, Herrmann H and Silberhorn C 2017 *npj Quantum Inf* **3** 5

[22] Shi B S and Tomita A 2004 *Phys. Rev. A* **69** 013803

[23] Kim T, Fiorentino M and Wong F N C 2006 *Phys. Rev. A* **73** 012316

[24] Fedrizzi A, Herbst T, Poppe A, Jennewein T and Zeilinger A 2007 *Opt. Express* **15** 15377

[25] Medic M, Altepeter J B, Hall M A, Patel M and Kumar P 2010 *Opt. Lett.* **35** 802

[26] Jabir M V and Samanta G K 2017 *Sci. Rep.* **7** 12613

[27] Graham R and Haken H 1968 *Z. Phys.* **210** 276

[28] Santandrea M, Stefszky M, Roeland G and Silberhorn 2019 *New J. Phys.* **21** 123005

[29] Helmfrid S and Arvidsson G 1991 *J. Opt. Soc. Am. B* **8** 797

[30] Clauser J F, Horne M A, Shimony A and Holt R A 1969 *Phys. Rev. Lett.* **23** 880

[31] James D F V, Kwiat P G, Munro W J and White A G 2001 *Phys. Rev. A* **64** 052312